ICAT 2001
December 5-7, Tokyo, Japan
THE VIRTUAL REALITY SOCIETY OF JAPAN

A Vision-based Tactile Sensor

Kazuto Kamiyama, Hiroyuki Kajimoto, Masahiko Inami, Naoki Kawakami, Susumu Tachi

1) The University of Tokyo,
7-3-1 Hongo, Bunkyo-ku, Tokyo, 113-8656 Japan
{ *kazuto, kaji, minami, kawakami, tachi* } *@star.t.u-tokyo.ac.jp*

Abstract

Receiving tactile information from a slave-robot is a necessary component of telexistence with haptic display, but there are few tactile sensors that can measure the distribution of three-dimensional force vectors on a surface. For this reason, we developed a sensor that provides three-dimensional force distribution by detecting movement vectors in the transparent elastic body with a video camera. From a result of the experiment, it turned out this approach is effective.

Key words: Telexistence, Tactile Sensor, Vision based, Force Vector

1. Introduction

As humans we affirm our own existence through tactile information, and true reality is unobtainable without the sense of touch. Because of that, displaying tactile information is a critical aspect in virtual reality. There has been extensive research on various types of haptic displays, such as mechanical by Iwata [1], electrical stimulation by Kajimoto [2], and so on, but in telexistence, technology that allows us to feel as if we exist in a distant place, sensing tactile information from a slave-robot is also a necessary and important aspect. While tactile displays and sensory input devices are related for telexistence, relatively few current tactile sensors can obtain sufficient information for tactile display. In this paper, we address tactile sensors that receive tactile information, which is necessary and sufficient for haptic display.

By establishing the purpose of our sensor as a tool to collect tactile information for haptic display, this solicits several capabilities. First, the direction of force on the surface of the sensor should be measured as well as its strength, because the fingertip can perceive both the distribution and direction of force at the same time. Second, this tactile sensor needs to have elasticity, since there exists an interaction between the sensor and the object being touched, whereas there is no such interaction in vision. When a finger touches an object, it applies force to the object, and it thereby gives rise to a certain influence to the object. Conversely, the reaction force from an object works on the finger as well, and the finger is influenced by the object in the form of variation. If this condition of mutual influence cannot be represented, the resulting tactile information will take on a different form from that of an actual finger.

There are few tactile sensors which fulfill both points that the three-dimensional vector distribution can be measured and also have the property of elasticity. Considering the first point, although a six-dimensional force sensor is already commercially available, as well as others such as a force vector of a single point, or a film force sensor that measures the distribution of force magnitude, few have the ability to measure the distribution of a three-dimensional force vector. A few can sense the vector distribution [3], but it is difficult to have arbitrary elasticity due to the complexity of the architecture. Here, we propose a new optical tactile sensor for displaying tactile information, which can measure a three-dimensional vector distribution and also has the property of elasticity.

2. Theory

The tactile sensor which we propose uses a transparent elastic body and a CCD camera. By photographing a certain marker on the interior of an elastic body by CCD, when force is applied to the surface, the variation information of the interior is measured, and is used to reconstruct a force vector distribution.

Various methods can be considered to acquire variation information. Our current approach is to measure the horizontal movement of the markers in the elastic body, which are located in an $N \times N$ array at a specified depth. To gather sufficient information for the reconstruction of the force vectors, we used two layers of markers that are located at different depths (Fig.1). These layers could be distinguished by the colors of the markers (red and blue). We set the x-y plane parallel to the sensor surface and the z axis extending vertically on the interior. By measuring these markers from a positive z direction with a CCD camera, we could obtain two sets of two-dimensional movement vectors at different depths, so the amount of information is increased and the distribution of force vector can be readily obtained.

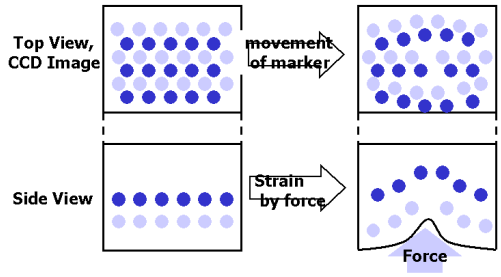

Fig. 1: Image of Sensing

2.1 Method of measuring position of markers

The $N \times N$ spherical markers in the elastic body described above are arranged in two planes at different heights parallel to the surface, with red markers at a certain height $z = a$ and blue markers at another height $z = b$, and a picture is taken of the internal reflection of these markers. It is possible to separate the information of markers at different heights by storing the picture in a 24-bit bitmap file, and extracting its red and blue components.

We explain the method of determining the center of the marker position. For computational purposes, the position of the picture is expressed as a matrix, and the optical density information for each pixel in the picture is expressed as a matrix element with a scalar value. A center of mass measurement method is performed to pinpoint the marker center position. First, the picture is divided into a mesh for every dozen pixels, which means carving an image matrix, and the center of mass of this mesh is calculated. The mesh is then divided again, focusing on the center of mass, and the center is recalculated. The center of mass calculated on this second pass establishes the center of the markers (Fig.2). This position, which was originally an integer value based on a pixel unit, becomes a real number with sub-pixel accuracy. Moreover, since the markers can be arranged in arbitrary positions and recalibrated with this marker center position determination method, camera alignment is no longer a strict requirement.

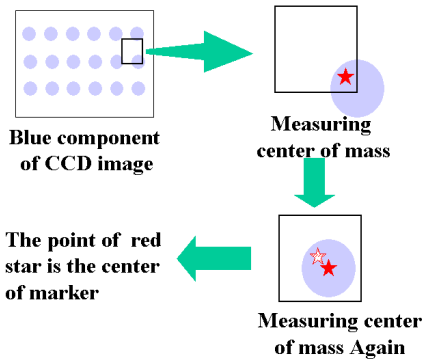

Fig. 2: Measuring The Center of Marker

2.2 Measuring distribution of two dimensional movement vector of markers

When force is applied to the elastic body surface, the markers move, and this movement is observed by the CCD. The picture is subdivided into partial squares, each of which is centered on the marker position measured in the previous state that force is not applied. By taking the difference of the position of the center in the picture before and after the movement, the markers' translation in the xy direction can be calculated. In this case, however, it is possible to measure movement only within the divided area. If necessary, so-called 'tracking' method can be applied, which only uses two sequential images.

2.3 Obtaining distribution of three dimensional force vector from movement vectors

In order to obtain a force vector from a movement vector, we use the theory of elasticity [5] by assuming that the elastic body is half-spaced, uniform and has linearity. We set z-axis perpendicular to the elastic body's interior surface, and the xy-plane parallel to the surface of the elastic body. Following Eq.2,Eq.1 express the movement vector $\vec{u} = (u_x, u_y)$ of the interior point $\vec{r} = (x, y, z)$ within a plane parallel to the xy-plane when a force vector $\vec{f} = (f_x, f_y, f_z)$ is applied to the surface of the elastic body. σ is a Poisson ratio, which is set to 0.5, by assuming that the elastic body is incompressible considers an ideal elastic body as incompressible, and is set to 0.5. E is Young's modulus and must be appropriately defined according to the actual elastic body used, but from this equation it is apparent that E is in effect only multiplying constant to the whole equation, so it is set to 1 here.

$$u_x = \frac{1+\sigma}{2\pi E}\left\{\left[\frac{xz}{r^3} - \frac{(1-2\sigma)x}{r(r+x)}\right] f_z + \frac{2(1-\sigma)r+z}{r(r+z)} f_x + \frac{[2r(\sigma r+z)+z^2]x}{r^3(r+z)^2}(xf_x + yf_y)\right\}, \quad (1)$$

$$u_y = \frac{1+\sigma}{2\pi E}\left\{\left[\frac{yz}{r^3} - \frac{(1-2\sigma)y}{r(r+x)}\right] f_z + \frac{2(1-\sigma)r+z}{r(r+z)} f_y + \frac{[2r(\sigma r+z)+z^2]y}{r^3(r+z)^2}(xf_x + yf_y)\right\} \quad (2)$$

From these equations, when unit force $\vec{f} = (f_x, f_y, f_z) = (1,0,0),(f_x, f_y, f_z) = (0,1,0),(f_x, f_y, f_z) = (0,0,1)$ is applied in each direction x,y,z, the movement vector of the point in the plane at certain depth $z = z_1$ is calculated. We represent it by u_{fx}=(h_{xx1}, h_{yx1}), u_{fy}=(h_{xy1}, h_{yy1}), u_{fz}=(h_{xz1}, h_{yz1}). These movement h can be considered as an impulsive response to unit force of each direction from the origin. When the force applied to the surface of the elastic body is reconsidered as a vector distribution expressed as $\vec{f}(x,y) = (f_x(x,y), f_y(x,y), f_z(x,y))$, the movement vector $\vec{m_1}(x,y) = (m_{x1}(x,y),\ m_{y1}(x,y), m_{z1}(x,y))$ in point (x,y) in the plane at a certain depth and is calculated in the form of convolution (Eq.3). Note that we utilized our assumption of linearity (the asterisk denotes convolution).

$$
\begin{aligned}
m_{x1}(x,y) &= h_{xx1} * f_x + h_{xy1} * f_y + h_{xz1} * f_z, \\
m_{y1}(x,y) &= h_{yx1} * f_x + h_{yy1} * f_y + h_{yz1} * f_z, \quad (3)
\end{aligned}
$$

A discrete form of this can be expressed as a matrix representation. The movement vectors and force vectors are sampled at $M \times N$ points, and the x, y, z components of the movement vector are expressed as M_{x1}, M_{y1}, M_{z1} in the matrix. Elements from $(1,1)$ to (M,N) are renumbered using one suffix and are reinserted as a vector. Stress vectors are inserted in the same fashion. By doing so, Eq.3 represents the matrix form (Eq.4).

$$
\begin{bmatrix} M_{x1} \\ M_{y1} \end{bmatrix} = \begin{bmatrix} H_{xx1} & H_{xy1} & H_{xz1} \\ H_{yx1} & H_{yy1} & H_{yz1} \end{bmatrix} \begin{bmatrix} F_x \\ F_y \\ F_z \end{bmatrix} \quad (4)
$$

As this equation calculates movement of an interior point when a force vector distribution is applied to the surface of the elastic body, its inverse becomes a formula which calculates the force vector distribution by giving the measured value M (Eq.5). This is the measurement principle of this research.

$$
F = H^{-1}M \quad (5)
$$

At this point, consider the number of M vector elements on the left side of the equation and the F vector elements on the right side. Since a number of sampling point is $M \times N$, the number of elements of a movement vector is $M \times N \times 2$ and the number of elements of a force vector is $M \times N \times 3$. It means that there are more unknowns than equations, which complicates the determination of the unknowns. Thus, the technique (stated in Section 2.1) of measuring in another height by using the color information is applied. As the impulse response is different in another height, we obtain the following equation.

$$
\begin{bmatrix} M_{x1} \\ M_{y1} \\ M_{x2} \\ M_{y2} \end{bmatrix} = \begin{bmatrix} H_{xx1} & H_{xy1} & H_{xz1} \\ H_{yx1} & H_{yy1} & H_{yz1} \\ H_{xx2} & H_{xy2} & H_{xz2} \\ H_{yx2} & H_{yy2} & H_{yz2} \end{bmatrix} \begin{bmatrix} F_x \\ F_y \\ F_z \end{bmatrix} \quad (6)
$$

This becomes a situation with more equations than unknowns, so it is easy to calculate a force vector distribution F. Since the matrix H is not a regular matrix, there does not exist an inverse matrix. Therefore, force will be calculated using a pseudo-inverse matrix. The pseudo-inverse matrix is briefly explained from relation of content in this paper.

The pseudo-inverse matrix is obtained using a method of least squares. The prediction error is set as e, and the connection between F and e is as follows:

$$
M = HF + e \quad (7)
$$

To determine the value F that minimizes the absolute value $\|e\|$ of error, this is rewritten into an equation (Eq.8) regarding error.

$$
\begin{aligned}
\|e\|^2 &= \|M - HF\|^2 \\
&= \frac{1}{2}F^T Q F + cF + d \quad (8)
\end{aligned}
$$

$$
Q = 2H^T H, c^T = -2M^T H, d = M^T M \quad (9)
$$

F should be the value that minimizes this prediction error. Hence, by differentiating Eq.8 by F, we obtain

$$
\begin{aligned}
(H^T H)F - 2c &= 0 \\
F &= (H^T H)^{-1} c \quad (10)
\end{aligned}
$$

2.4 Algorisms of improving stability

Because noise will be contained in the measurement of motion, we use an algorithm for enhancing the stability of calculating the force vector distribution in the presence of noise. This adds certain constraints to the method of least squares that was explained above.

2.4.1 Constraint of minimizing norm of difference between adjacent force vectors

By assuming the spatial distribution of a force vector does not change steeply, we impose a constraint that minimizes the norm of the difference between the adjacent force vector. The equation is as follows.

$$
\begin{aligned}
\|\Delta F\|^2 &= \|F(1) - F(2)\|^2 + \|F(2) - F(3)\|^2 \\
&\quad + \|F(3) - F(4)\| + ... \\
&= \left\| \begin{bmatrix} 1 & -1 & 0 & \dots & 0 \\ 0 & 1 & -1 & \dots & 0 \\ 0 & 0 & 1 & \dots & 0 \\ \vdots & & \ddots & & \vdots \\ 0 & 0 & \dots & 1 & -1 \end{bmatrix} F \right\|^2 \quad (11) \\
&= F^T Q_2 F
\end{aligned}
$$

By combining with Eq.8 and setting the weight value ω.

$$
minimize \left\{ \frac{1}{2}F^T (Q + \omega Q_2) f + cF + d \right\}
$$

then,

$$
F = (H^T H + \frac{1}{2}\omega Q_2)^{-1} c \quad (12)
$$

2.4.2 Constraint that the value of z-direction is positive

Unless an adhesive object is measured, we could assume that the z-direction component of the force is a positive value, which requires an additional constraint.

$$
minimize \left\{ \frac{1}{2}F^T Q F + cF + d \mid F_z \geq 0 \right\} \quad (13)
$$

In this case, a least squares method such as Eq.8 using pseudo-inverse matrices is no longer applicable, and it becomes a quadratic programming problem requiring an iterative approach, so the amount of calculation will increase.

2.4.3 Constraint of minimizing norm of force vectors

The force applied to an elastic body is limited, so an additional constraint is added so that the calculated power vector may not diverge. It is formulated as follows, with I as the identity matrix, and like the constraint to minimize the norm of difference between adjacent force vectors, it can unite with Eq.8 and is written as follows.

$$\begin{aligned} \|F\|^2 &= \|F(1)\|^2 + \|F(2)\|^2 + \|F(3)\| + ... \\ &= F^T I F \end{aligned} \tag{14}$$

$$minimize \left\{ \frac{1}{2} F^T (Q + \omega I) F + cF + d \right\} \tag{15}$$

2.5 Camera caribration

The method proposed in this research will reconstruct force vector distribution from the two-dimensional movement vector in a plane of the elastic body surface. The reason for this is that the picture taken by CCD is two dimensional, but the photograph does not only show movement in the plane perpendicular to the axis of the CCD lens. This is based on the lens characteristic of a CCD camera and like Fig.3 the motion of z-direction, which should be originally calculated with no movement, will be detected as movement in the xy direction in the form projected. However, a picture does not in fact show whether movement of a marker is in the xy direction or the z direction. Therefore, the impulse response currently used in Eq.3 must be corrected by including the projection of the z-directional motion to the xy-plane.

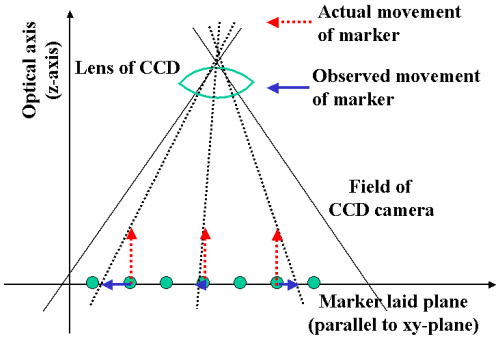

Fig. 3: Necessity to caribrate image of CCD camera

3. Experimental setup

The system of the sensor created this time is shown in Fig.4.

A black shading layer is prepared in the surface of the transparent elastic body of a height of 40mm, 90mm long,

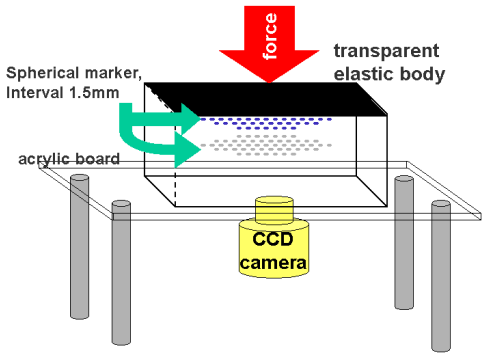

Fig. 4: Image of sensor system

and 100mm wide. We uses silicone rubber (Shin-Etsu Chemical Co.,Ltd. KE109) as the transparent elastic body. The elastic body must be large enough to satisfy the half-space assumption. It resulted into this size.

Blue markers are arranged at 3mm in depth and red markers at 6mm in depth. The marker interval is about 1.5mm. Markers are arranged at the interval suitable for man's limit of spatial resolution that he can discriminate between two separated point. The markers needs to be so small that assumption of an uniform elastic body does not collapse and the markers of different depth do not overlap with each other as much as possible. At the same time, they also needs to be large enough so that the center of marker can be calculated to sub-pixel and the diameter of a ball occupy some pixels of pictures taken by CCD. The size of markers are adjusted so that they might be filled. We uses the plastic ball (DAICEL FINECHEM, LTD. FREEPLASTIC) as color marker.

The markers inside the elastic body are photographed through the transparent acrylics board which fix the elastic body (Fig.5). One pixel corresponds to about 0.05mm. The image is outputted by NTSC format and sent to PC through the capture unit of USB connection.

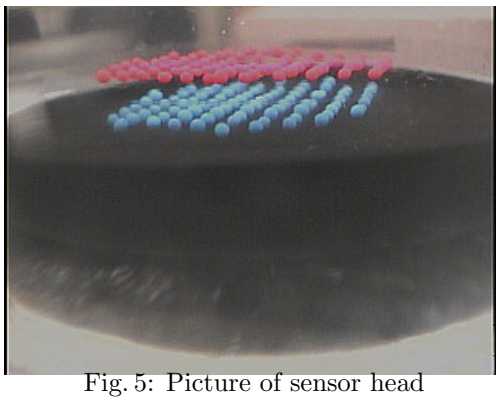

Fig. 5: Picture of sensor head

4. Experiment

4.1 Picturize marker

The picture taken by CCD is shown Fig.6. We extracted Red and Blue component of the picture so that we could separately obseve the markers with different depth. For noise reduction, the picture is preprocessed by taking diffrence of Red and Blue component. Positive part of this differennce is considered as Red component, and negative part is regarded as Blue component.

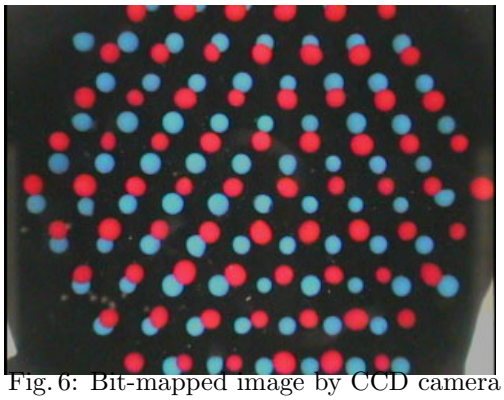

Fig. 6: Bit-mapped image by CCD camera

4.2 Measuring movement vector

First, we evaluated accuracy of our algorism of calculating the movement vector. A photographed picture when force was not applied was considered as original one before markers moving and another picture, which was displaced at 3 pixel on the right, as one after markers move. We used these images and calculated the movement vector of a marker (Fig.9). Each histgram of Red,Blue component of x, y-direction element of movement vector are Fig.8. Their average and standard deviation is shown Table1.

Fig.9 is the movement vector distribution of Red component when applying z-direction force which is perpendicular to surface of elastic body using a pillar with a diameter of 5mm. As the elastic body deforms radially, the obtained movement vector looks as a projected image of this radiation pattern.

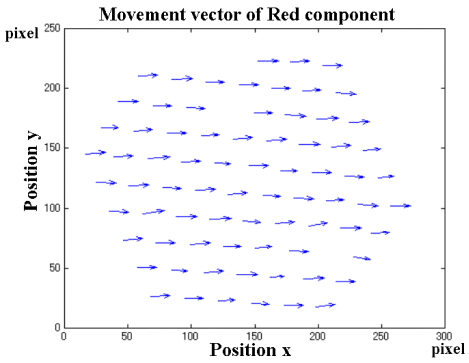

Fig. 7: Calculate movement vector using shifted image

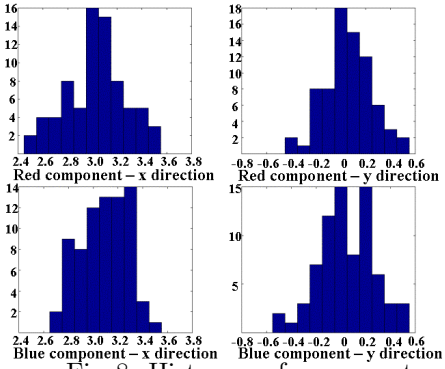

Fig. 8: Histgram of movement

Table 1: Test of Measuring movememt

Component	direction	Average(Pixel)	SD
Blue	x	3.09	0.19
	y	0.05	0.22
Red	x	3.02	0.25
	y	0.06	0.19

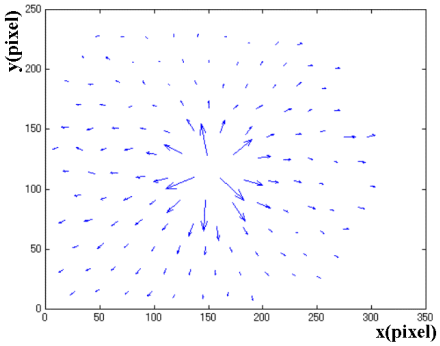

Fig. 9: Calculate movement vector when given z-directional force

4.3 Reconstructing force vector

In this subsection, force vector is reconstructed in two situations. One is when only vertical force is applied, and the other is when horizontal force is also applied.

4.3.1 Reconstruction of force vector when only z-direction force applied

Following is the result of force vector reconstruction when the force is applied perpendicularly to the surface using pillar which diameter is 5mm. During calculation, three constraints that are explained in section 2 are applied.

The result calculated without any constraints has been diverged greatly. A very big value is obseved at the point clearly different from the point of applied force. When constraint of minimizing norm of difference between adjacent force vectors (Eq.11) is imposed, an obtained result is Fig.10. When other constraint of minimizing norm of force vectors (Eq.14) is imposed, Fig.11 is reconstracting result. Because iteration doesn't exist in these two constraint, calculation time is short and it took about 0.08

sec from the capture of the picture until it returned the result.

On the contrary, constraint that the value of z-direction is positive accompanied with the constraint of minimizing norm of difference between adjacent force vectors is imposed (Eq.13), obtained result is Fig.12. This algorithm includes iterate calculation during force vector is reconstructed, so that calculation speed is slower than the two above-mentioned algorithms and it took about 0.9 sec.

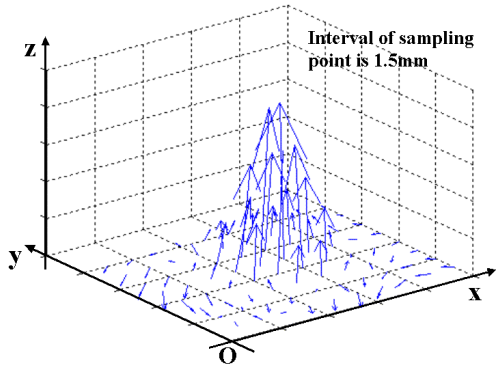

Fig. 10: Distribution of force vector:minimizing norm of difference

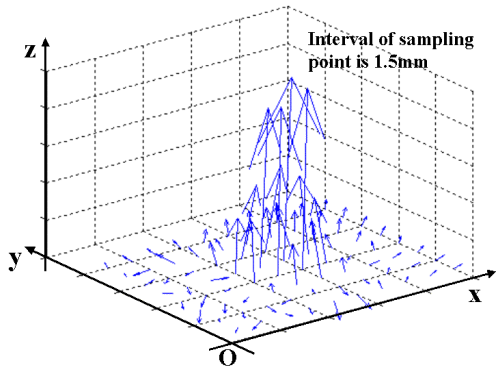

Fig. 11: Distribution of force vector:minimizing norm of vector

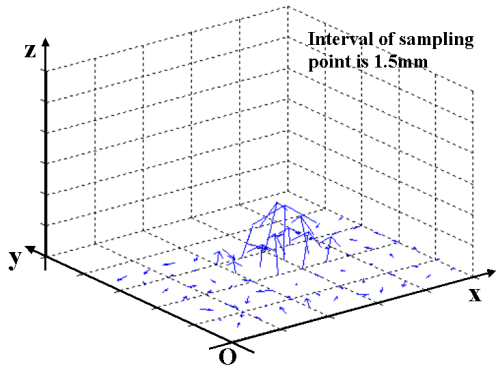

Fig. 12: Distribution of force vector:positive z-direction value

These three figures of results was obtained after calibrating data from CCD camera which we described in Section 2.5. The result without this calibration when constraint of minimizing norm of force vectors is applied, is shown in Fig.13.

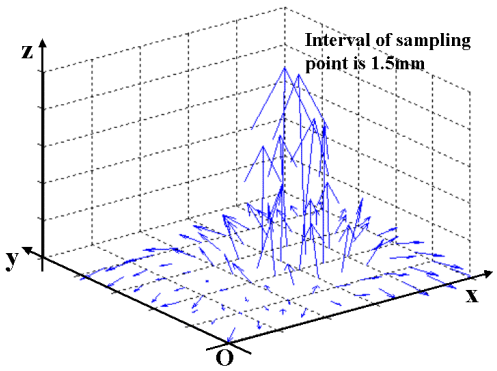

Fig. 13: Distribution of force vector:minimizing norm of vector,before camera caribration

Next, the experiment which investigates spatial resolution was conducted. force is applied equally along with a y-axis using square pillar. Then distribution of z-component of the force vector along with an x-axis is investigated while pushing in the direction of z. The measurement was conducted for every different length of the side of square pillar along with the x-axis. Fig.14 is the result.

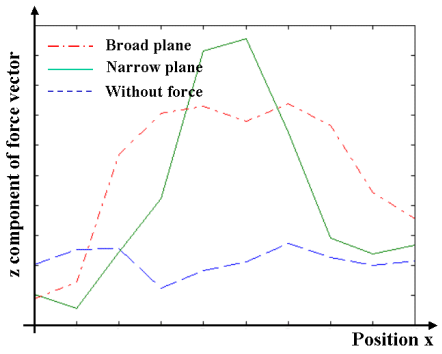

Fig. 14: Applying force with various width of plane

4.3.2 Reconstruction of force vector distribution when three-dimensional force applied

When force in the direction of z and twist around z-axis is applied using the pillar with a radius of 20mm on the elastic body, reconstructed distribution of force vector is shown in Fig.13.

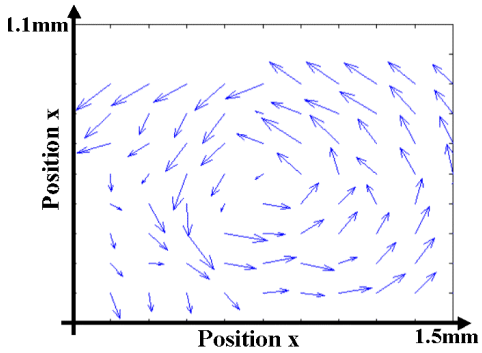

Fig. 15: Applied torque arround z-axis

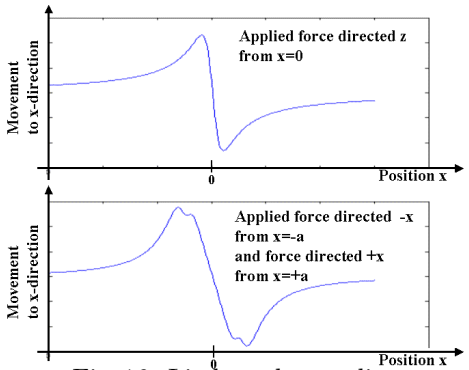

Fig. 16: Little orthogonality

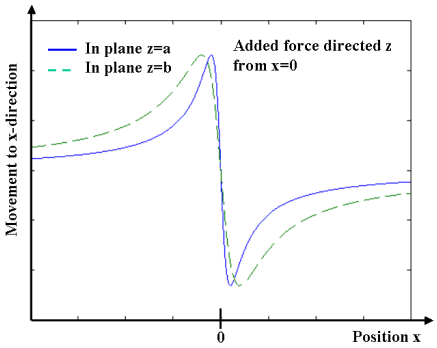

Fig. 17: Changes of movement in hight difference

5. Speculation

In this section, We discuss about movement vector measurement, reconstruction of force vector distribution and spacial resolution.

5.1 Accuracy of measuring movement vector

From Table1, It turned out that the obtained movement vector has about $\pm$ 0.4-pixel data spread at the maximum from histgram (Fig.8). The maximum value of a movement vector is about 10 pixels. Herewith, data spread of about $\pm$ 0.4-pixel never means small and it is never able to said to measure accurately. We have to measure the movement vector with sufficient accuracy from the following three points.

1. Because the data actually measured is movement and force vector which is a needed quantity is calculated from its data, accuracy of force vector better than the accuracy of a movement vector is never achieved.
2. While force was applied from various directions, in a rare case some force vectors with completely incorrect direction were observed. It turned out that the reason was inaccurite movement vector around the obtained force. As it was thought that the correctly calculated movement vector compensate this inaccurate one, it figure out that there is almost no robustness to error from mistaken calculation.
3. Like Fig.16, addition of only two impulse responses of the x-direction makes quite the same movement that unit force of z-direction on origin was applied. Regarding each movements of the impulse response to unit force of the direction of z,x and y as basis function in equation of convolution, they are not orthogonal but nearly pallarel to each other. Additionally, the impulse response in a certain height and the other response in different height are not also orthgonal basis function (Fig.17).

5.2 About calculating distribution of force vector

It is called inverse analysis to calculate force vector from movement vector. There are many reserch about inverse analysis[6]. When there are more unknowns than the number of simultaneous equations, it is called underdetermined problem. On the contrary, the problem that there are less unknowns than equations is called overdetermined problem. Our approach was to change problem from underdetermined to overdetermined by using two observation layers.
constraint of minimizing norm of difference between adjacent force vectors and of minimizing norm of force vectors respectively result from 'smoothness of a solution','simplicity of a solution' and they applied when including underdetermined problem. As the foregoing subsection described, the overdetermined part in problem is buried in a noise and is very weak. Therefore, it is thought suitable to add such constraint.

6. Conclusion

As discussed in section 1, our purpose of tactile sensor is realization of an artificial tactile sensation. From this point, spacial resolution and response speed of the sensor need to be better than these of human. We compare fingertip of humans about this point with the tactile sensor manufactured in this research.

First, it is reported that the spatial resolution of the human's fingertip is 2mm. Although the sensor in our reserch has not yet attained to this ability, we expect to achieve this resolution by raising the measurment accuracy of movement vector with a closer interval between markers than the present. Unlike a mechanical sensor, only a colored marker with spherical shape is needed, so

a higher density of markers is easily attained.

The second point is the speed of response. Without quadratic programming, the current calculation time of our sensor on an Intel Pentium4 1.8GHz PC is 0.08sec. The bottlenecks are image capture and noise reduction, which take 0.03sec and 0.02sec, respectively. The firing frequency of the mechanorecepters of a human fingertip is tens of Hz in Meissner corpuscle and Merkelcell, 200Hz in Pacini corpuscle. The Missner corpuscle perceives low freqency vibration, and the Merkel cell perceives displacement of skin. They exist in high density. On the contrary, the Pacini corpuscle, which detects high-frequency vibration, exists in low density. We compensate for the role of the Pacini corpuscle with another tactile sensor, which is unable to be arranged in high density but has a quick response. The goal for our sensor is to sufficiently cover the domain in which the Missner corpuscle and the Merkel cell fire, and a rate of 70 Hz would be preferable. We believe our sensor can meet the speed of this domain through software optimization.

Future work includes overcoming these engineering hurdles to allow the development of a sensor with the capacity of the human's tactile sense. In addition, we will develop a finger shaped tactile sensor, which is our final target.

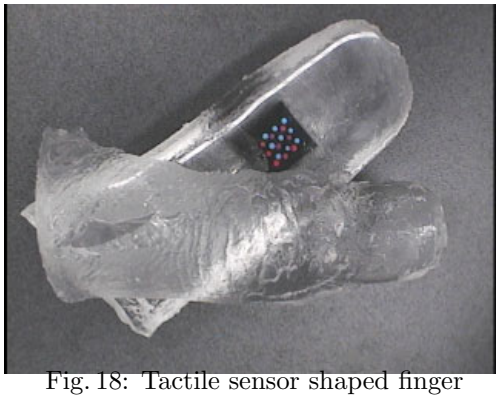

Fig. 18: Tactile sensor shaped finger

References

1. R.Kawamura, H.Yano, H.Iwata. "Development of surface type haptic interface for presentation of rigidity distribution", Proceedings of the Virtual Reality Society of Japan, 5 pp.51-54, 2000.
2. H.Kajimoto, N.Kawakami, T.Maeda, S.Tachi, "Tactile Feeling Display using Functional Electrical Stimulation", The Ninth International Conference on Artificial reality and Telexistence, pp.107-114, 1999.
3. M.Ohka, Y.Mituya, K.Hattori, I.Higashioka. "Data conversion capability of optical tactile sensor featuring an array of pyramidal projections", IEEE International Conference on Multisensor Fusion and Integration for Intelligent Systems, pp.573-580, 1996.
4. K.Tanie, K.Komoriya, M. Kaneko, S.Tachi, "A HIGH RESOLUTION TACTILE SENSOR", proceedings of the 4th international conference on robot vision and sensory controls, pp.251-261, 1987.
5. L.D.Landau,E.M.Lifshitz. "Theory of Elasticity", BUTTERWORTHHEINEMANN, 1985.
6. William Menke. "Geophysical Data Analysis: Discrete Inverse Theory", Academic Press, Inc., 1989.
7. R.S.Fearing, "Using a Cylindrical Tactile Seosor for Determining Curvature", IEEE Trans. on Robotics and Automation, vol.7, No.6, pp.806-817, 1991.